ADVANCED MATERIALS
www.advmat.de

Dynamic and Tunable Threshold Voltage in Organic Electrochemical Transistors

Sean E. Doris, Adrien Pierre, and Robert A. Street*

In recent years, organic electrochemical transistors (OECTs) have found applications in chemical and biological sensing and interfacing, neuromorphic computing, digital logic, and printed electronics. However, the incorporation of OECTs in practical electronic circuits is limited by the relative lack of control over their threshold voltage, which is important for controlling the power consumption and noise margin in complementary and unipolar circuits. Here, the threshold voltage of OECTs is precisely tuned over a range of more than 1 V by chemically controlling the electrochemical potential at the gate electrode. This threshold voltage tunability is exploited to prepare inverters and amplifiers with improved noise margin and gain, respectively. By coupling the gate electrode with an electrochemical oscillator, single-transistor oscillators based on OECTs with dynamic time-varying threshold voltages are prepared. This work highlights the importance of electrochemistry at the gate electrode in determining the electrical properties of OECTs, and opens a path toward the system-level design of low-power OECT-based electronics.

Since the first literature report of an organic electrochemical transistor (OECT) in 1984,[1] there has been an explosion of publications highlighting the applications of OECTs in chemical sensing,[2–5] biosensing and interfacing,[6–11] neuromorphic computing,[12–15] digital logic,[16–19] and printed electronics.[20–22] These applications of OECTs are enabled by their low operating voltage, compatibility with aqueous solutions and biological systems, and high transconductance. Despite these advantages, the incorporation of OECTs in practical electronic circuits is limited by the relative lack of control over their threshold voltage, which is important for controlling the power consumption and noise margin in complementary and unipolar circuits.[23,24] In this work, the threshold voltage of OECTs is precisely tuned over a range of more than 1 V by chemically controlling the electrochemical potential at the gate electrode. This threshold voltage tunability is exploited to prepare inverters and amplifiers with improved noise margin and gain, respectively. By coupling the gate electrode with an electrochemical oscillator, single-transistor oscillators based on OECTs with dynamic time-varying threshold voltages are prepared. This work highlights the importance of electrochemistry at the gate electrode in determining the electrical properties of OECTs, and opens a path toward the system-level design of low-power OECT-based electronics.

OECTs consist of a redox-active channel material separated from a gate electrode by an ionically conductive electrolyte (**Figure 1**a). Upon the application of a gate voltage, charge in the external circuit flows between the source and gate as the oxidation state (and the doping level) of the channel material is changed, leading to a change in the channel conductance.[25–27] The circuit is completed by the movement of ions in the electrolyte, which provide charge compensation for the newly injected carriers in the channel and participate in an oxidation (for positive gate voltage) or reduction (for negative gate voltage) reaction at the gate. The performance of OECTs can be tuned by controlling the device geometry and configuration[28–31] as well as through the design of channel materials with high carrier mobility and ionic conductivity.[32–35] These studies typically focus on transconductance, on/off ratio, and switching speed as metrics for device performance. In addition to these parameters, the transistor's threshold voltage (V_T)—the voltage at which the transistor switches on—is critical in the design of circuitry as it dictates the noise margin of digital logic and the power consumption of circuits.[23,24] Despite its importance for OECTs, relatively little attention has been paid to controlling their threshold voltage or to the role of electrochemistry at the gate electrode.[11,30,36,37] To address this critical knowledge gap, we hypothesized that the threshold voltage of OECTs could be tuned by controlling the electrochemical potential at the gate electrode (Figure 1b) in much the same way that the threshold voltage in electrolyte-gated transistors can be tuned by controlling the gate's work function.[38,39]

As shown in Figure 1b, the electrochemical potential in the channel is a function of the doping level, and the applied gate voltage (V_G) required to achieve a given level of doping depends on the electrochemical potential at the gate. Thus, the transfer curve (and as a result, the threshold voltage) for an OECT can be shifted by changing the electrochemical potential at the gate. This hypothesis was tested by preparing gate electrodes consisting of a metal (either inert or redox-active) in contact with a wide variety of dissolved redox-active species (Table S1,

Dr. S. E. Doris, Dr. A. Pierre, Dr. R. A. Street
Palo Alto Research Center—a Xerox Company
3333 Coyote Hill Road, Palo Alto, CA 94304, USA
E-mail: Sean.Doris@parc.com

The ORCID identification number(s) for the author(s) of this article can be found under https://doi.org/10.1002/adma.201706757.

DOI: 10.1002/adma.201706757

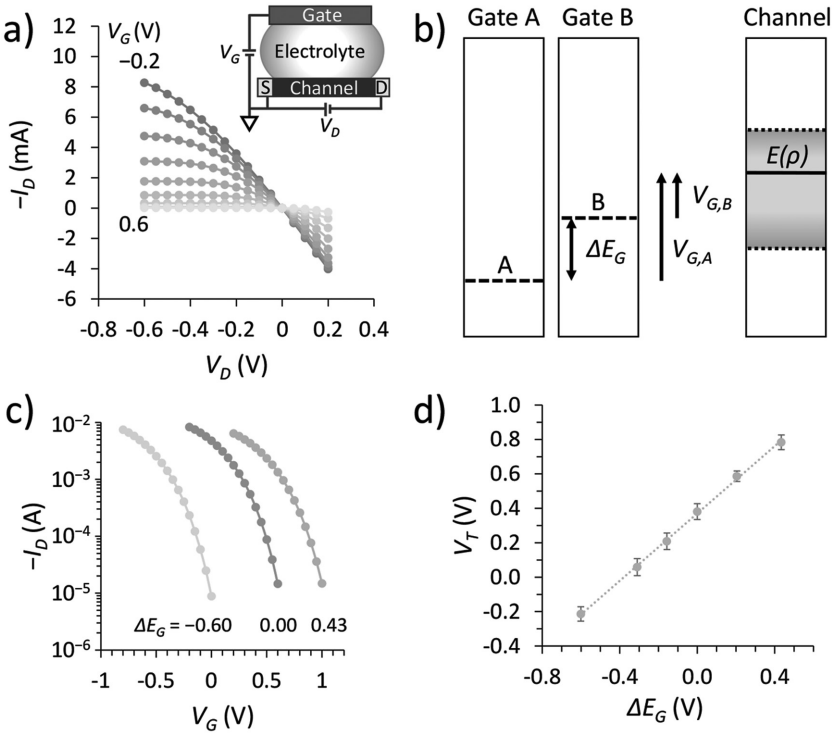

Figure 1. Tuning the threshold voltage of OECTs by controlling the electrochemical potential at the gate. a) Output curves for a 100 × 10 µm PEDOT:PSS OECT. V_G was stepped from −0.2 to 0.6 V in 0.1 V increments. (the inset) schematic of an OECT; b) energy level diagram for two OECT gates with different electrochemical potentials illustrating the role of gate electrochemical potential in determining the electrical properties of OECTs. The electrochemical potential in the channel, $E(\rho)$, is a function of doping level, and the applied gate voltage required to reach an arbitrary doping level depends on the electrochemical potential of the gate. The gate electrochemical potential (ΔE_G) is defined with respect to the commonly used Ag/AgCl reference electrode; c) transfer curves (V_D = −0.6 V) for a 100 × 10 µm PEDOT:PSS OECT are shifted by hundreds of millivolts when they are paired with gates of differing electrochemical potentials; d) threshold voltage, V_T, as a function of gate electrochemical potential.

Supporting Information) in order to establish a stable, well-defined electrochemical potential at the gate. In order to study the effect of the gate electrochemical potential on the behavior of OECTs, it was necessary to ensure that the channel electrochemistry and device capacitance were not also changed upon changing the gate electrochemical potential. This was accomplished by making the gate electrodes much larger than the channel area to ensure that $C_{gate} \gg C_{channel}$ (so the device capacitance is dominated by the channel capacitance) and by separating the gate electrolyte from the channel electrolyte with a porous glass frit (so the channel electrolyte, and thus its electrochemical behavior, was the same for all gates; see Figure S1 in the Supporting Information). As shown in Figure 1c, the transfer curves for OECTs prepared with poly(3,4-ethylenedioxythiophene) polystyrene sulfonate (PEDOT:PSS) channels were shifted by hundreds of millivolts when they were paired with gates of different electrochemical potentials. This effect was quantified by extracting the threshold voltage (V_T, see Figure S2 in the Supporting Information) from the transfer curves and plotting it as a function of the gate electrochemical potential with respect to Ag/AgCl (ΔE_G). As shown in Figure 1d, the threshold voltage scales linearly ($R^2 > 0.999$) with the gate electrochemical potential with a slope of 0.98 ± 0.04 V V^{-1} and an intercept, which will vary for different channel materials, of 0.37 ± 0.01 V. A wide range of gate electrochemical potentials from −0.60 to 0.43 V versus Ag/AgCl was accessible, meaning the behavior of PEDOT:PSS OECTs could precisely be tuned from depletion (V_T = 0.8 V) to enhancement-mode (V_T = −0.2 V) operation with no changes in the semiconductor material or its carrier mobility and subthreshold slope (Figure S3, Supporting Information). This allows the channel material to be optimized for high carrier mobility and ionic conductivity without regard for its threshold voltage, as the threshold voltage can be independently tuned by careful choice of gate material.

This threshold voltage tunability was exploited to improve the performance of digital and analog electronics. The inverter, which accepts a digital Hi or Lo signal and outputs the opposite signal, is among the simplest logic gates from which digital logic circuits can be prepared. In complementary logic circuits, inverters consist of an n- and p-type transistor in series sharing a common gate. This configuration allows for low-power logic with good noise margins and gain, but is only achievable if both n- and p-type transistors with comparable mobilities are available. Unfortunately, there is a relative dearth of n-type OECT materials, and those that are available do not match the high mobility of p-type PEDOT:PSS, which necessitates the use of unipolar logic.[34] While OECT-based unipolar inverters have been reported, they typically require multiple voltage rails or exhibit mismatched input and output voltage ranges, which greatly increases their complexity and difficulty of use in integrated circuits.[16,19] As shown in **Figure 2**, depletion-mode unipolar inverters with a single voltage rail and good noise margin can be prepared with if the threshold voltages of T_1 and T_2 are set to suitable values. This inverter design is enabled by the threshold voltage tuning described above, where the threshold voltages of T_1 and T_2 are both set to ≈−0.21 V. The voltage transfer characteristics for this inverter are excellent, with a peak gain of 20 V V^{-1} and a noise margin of 320 mV for a supply voltage of 800 mV, which is close to the maximum possible noise margin of 400 mV (Figure S4, Supporting Information). As n-type and ambipolar OECTs become available, the ability to tune their threshold voltage by tuning the electrochemical potential at the gate will be critical for fine-tuning the performance of OECT-based integrated circuits.

In addition to improving the performance and simplifying the design of digital logic, OECTs with tunable threshold voltage are also useful in analog circuits. As a prototypical circuit, we implemented an OECT as a common-source amplifier by placing the drain in series with a load resistor (Figure 2c).[40]

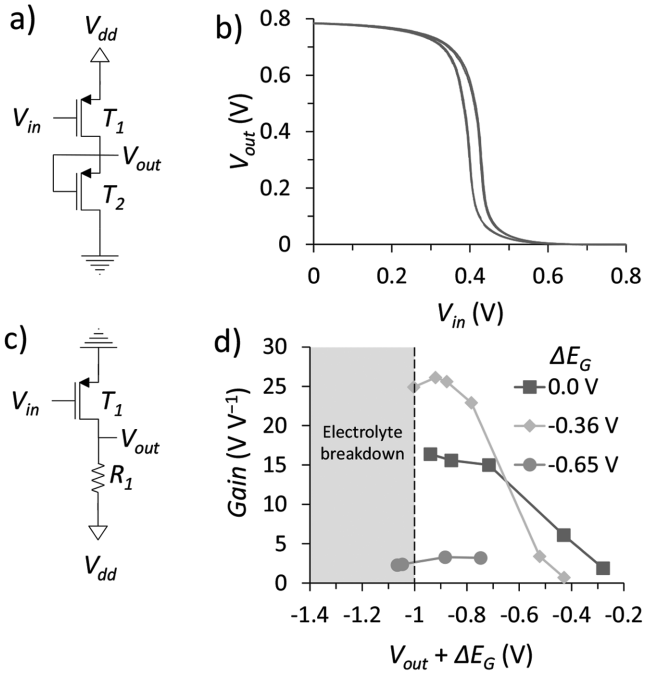

Figure 2. Applications of OECTs with tunable threshold voltage in digital and analog electronics. a) Simplified unipolar inverter design that is enabled by OECTs with tunable-threshold voltage; b) voltage transfer characteristic of the inverter depicted in panel (a) with V_{dd} = 0.8 V and $V_{T,T1} = V_{T,T2} = -0.21$ V; c) OECT-based common-source amplifier circuit;[40] and d) amplifier gain as a function of minimum channel electrochemical potential (vs Ag/AgCl) for OECTs prepared with different gates.

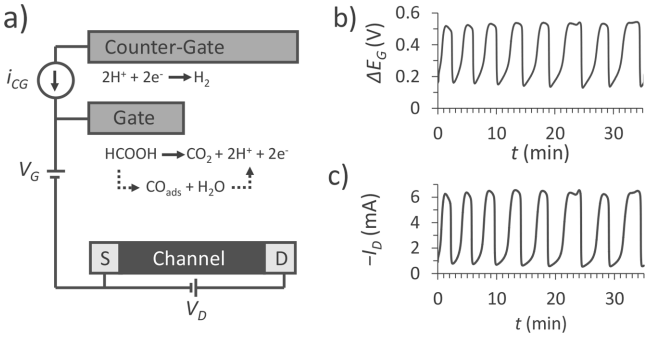

Figure 3. Dynamic threshold voltage OECT. a) Scheme of an OECT gated with an electrochemical oscillator. A DC current (I_{CG}) is driven between the gate and counter-gate electrodes, which induces electrochemical reactions to happen at the gate and counter-gate electrodes. The first step of the indirect pathway (dashed lines) inhibits the direct pathway, eventually forcing the system to proceed through the higher potential indirect pathway until the adsorbed CO is removed from the electrode surface; b) the electrochemical potential at the gate electrode (ΔE_G) oscillates as the gate electrochemical reaction alternates between two available pathways; c) the oscillation in gate electrochemical potential leads to an oscillation in OECT threshold voltage, giving oscillatory drain current when biased under DC conditions (V_G = 0.5 V and V_D = –0.6 V).

Many signals of interest, including bioelectrical signals from neurons, are small amplitude signals centered around 0 V, so it is useful to design high-gain amplifiers for signals without a DC offset. As described elsewhere,[40] the gain for the circuit depicted in Figure 2c is a function of the load resistance, channel differential resistance, and OECT transconductance. In practical systems the supply voltage (V_{dd}) is fixed by system-level considerations, while the minimum and maximum allowable voltages in the channel are set by the electrochemical stability of the channel material and electrolyte. While the exact electrochemical stability window for a channel and electrolyte will depend on the kinetics of electrolyte breakdown, a good rule of thumb for aqueous electrolytes is to ensure that the channel voltage always falls between –1 and 1 V versus Ag/AgCl. These constraints limit the achievable gain for practical systems, though tuning the transistor threshold voltage provides another knob for improving amplifier performance. To test the effect of threshold voltage on amplifier gain, we prepared the common-source amplifier depicted in Figure 2c with an OECT paired with gates of different electrochemical potentials and a –5 V supply rail. For each gate, we measured the gain, $\Delta V_{out}/\Delta V_{in}$, for a 10 mV peak-to-peak AC input signal centered around 0 V. The gain was measured with different load resistances, taking care that no part of the channel ever fell below the electrochemical stability limit of –1 V versus Ag/AgCl. This is the case whenever $V_{out} + \Delta E_G > -1$ V. As shown in Figure 2d, the maximum gain achieved with a Ag/AgCl gate (ΔE_G = 0.0 V, $V_T \approx 0.37$ V) was 16 V V^{-1}, while a higher gain of 26 V V^{-1} could be achieved with a gate electrochemical potential of ΔE_G = –0.36 V ($V_T \approx 0.02$ V). Further decreasing ΔE_G to –0.65 V ($V_T \approx -0.27$ V) led to a drop in gain to 3 V V^{-1}, demonstrating that there is an optimal threshold voltage for OECT-based voltage amplifiers. Simulation Program with Integrated Circuits Emphasis (SPICE) simulations with devices modeled after OECTs qualitatively matched this behavior (Figure S5, Supporting Information). In both analog and digital circuits, tuning the threshold voltage of OECTs by controlling the electrochemical potential at the gate electrode dramatically improved the performance and simplicity of OECT-based circuitry without the need for custom-designed channel materials.

Another advantage of tuning V_T by controlling the electrochemical potential at the gate electrode is that V_T can be dynamic—that is, V_T can vary with time. By coupling the gate electrode with electrochemical systems that exhibit oscillatory changes in electrochemical potential, known as electrochemical oscillators, single-transistor OECT oscillators can be prepared. This was accomplished by introducing a second electrode, coined the "counter-gate" electrode, into the gate electrolyte and driving a fixed current between the gate and counter-gate electrodes (**Figure 3**a). This application of current induces an electrochemical reaction to happen at the gate and counter-gate electrodes. If multiple electrochemical reactions are possible, then the reaction with the lowest activation barrier will proceed. Furthermore, if the electrochemical reactions are coupled (for example, the occurrence of one of the reactions changes the activation barrier for the other reaction), then it is possible to establish a system where the reaction pathway alternates between multiple available pathways. This leads to an oscillation in electrochemical potential at the gate and a concomitant oscillation in the OECT threshold voltage. As a demonstration of this concept, we prepared an OECT that used the widely studied electrochemical oscillator based on formic acid oxidation.[41,42] Platinum gate and counter-gate electrodes were immersed in a solution of

formic and sulfuric acid, and a constant current (I_{CG}) was driven between the two electrodes. This caused formic acid, HCOOH, to be oxidized to CO_2 and $2H^+$ at the gate electrode and $2H^+$ to be reduced to H_2 at the counter-gate electrode. Because the oxidation of formic acid can proceed through two competing pathways with cross-coupled kinetics, the electrochemical potential at the gate electrode oscillated as the dominant pathway changed (see the Supporting Information for more details). This caused the OECT threshold voltage to oscillate, leading to an oscillation in the drain current when the OECT was biased under DC conditions (V_G = 0.5 V, V_D = −0.6 V, I_{CG} = 2 µA). The oscillation of this device was much slower (f = 3.7 mHz) than typical ring oscillator circuits, which should have applications in long-term timing functionality as well as periodic sensor polling.

Controlling the electrochemical potential at the gate electrode is a powerful and previously underexplored strategy for controlling the threshold voltage of OECTs, which greatly improves their utility in printed electronics, biointerfacing, and sensing applications. Here, we showed that OECT threshold voltage can be tuned by chemically controlling the electrochemical potential at the gate. This strategy allows the OECT channel material to be optimized for high mobility and ionic conductivity without regard for threshold voltage, since the threshold voltage can be dialed into any desired value by tuning the gate electrochemical potential. By employing this strategy, we demonstrated simplified inverters with good gain and noise margin, amplifiers with improved gains, and single-transistor oscillators with applications in low-power sensor polling and printed electronics.

Experimental Section

OECTs with PEDOT:PSS channels and gold source/drain contacts were prepared as described in the literature[43] and in the Supporting Information. The OECTs were immersed in electrolyte (0.1 M NaCl) and separated from the gate electrode and electrolyte by a porous glass frit. The electrochemical potential of each gate with respect to the commonly used Ag/AgCl reference electrode (ΔE_G) was measured by measuring the open-circuit voltage between the two electrodes when they were both immersed in 0.1 M NaCl. The voltage-transfer characteristic of the inverter was measured by sweeping a 100 mHz triangular wave input signal and measuring the output voltage. The common-source amplifier was prepared with resistors ranging from 5 kΩ to 100 MΩ and a supply voltage of V_{dd} = −5.0 V. The input signal was a 5 Hz sinusoidal 10 mV peak-to-peak signal centered around 0.0 V. Electrochemical oscillators were prepared with a gate electrolyte consisting of 1.0 M formic acid in 0.5 M sulfuric acid. The gate electrode was a platinum disk electrode with a geometric surface area of 0.03 cm^2 and the counter-gate electrode was a platinum wire.

Supporting Information

Supporting Information is available from the Wiley Online Library or from the author.

Acknowledgements

The authors gratefully acknowledge funding from Xerox. The authors would also like to thank R. Lujan for assistance with device fabrication and J. Rivnay, W. Jackson, and P. Mei for helpful discussions.

Conflict of Interest

The authors declare no conflict of interest.

Keywords

organic electrochemical transistors, organic electronics, printed electronics, threshold voltage

Received: November 19, 2017
Revised: January 5, 2018
Published online: March 2, 2018

[1] H. S. White, G. P. Kittlesen, M. S. Wrighton, *J. Am. Chem. Soc.* **1984**, *106*, 5375.
[2] P. Lin, F. Yan, *Adv. Mater.* **2012**, *24*, 34.
[3] J. T. Mabeck, G. G. Malliaras, *Anal. Bioanal. Chem.* **2006**, *384*, 343.
[4] Z. Mousavi, A. Ekholm, J. Bobacka, A. Ivaska, *Electroanalysis* **2009**, *21*, 472.
[5] M. Sessolo, J. Rivnay, E. Bandiello, G. G. Malliaras, H. J. Bolink, *Adv. Mater.* **2014**, *26*, 4803.
[6] J. Rivnay, R. M. Owens, G. G. Malliaras, *Chem. Mater.* **2014**, *26*, 679.
[7] M. Berggren, A. Richter-Dahlfors, *Adv. Mater.* **2007**, *19*, 3201.
[8] D. T. Simon, E. O. Gabrielsson, K. Tybrandt, M. Berggren, *Chem. Rev.* **2016**, *116*, 13009.
[9] L. Kergoat, B. Piro, M. Berggren, G. Horowitz, M.-C. Pham, *Anal. Bioanal. Chem.* **2012**, *402*, 1813.
[10] D. Khodagholy, T. Doublet, P. Quilichini, M. Gurfinkel, P. Leleux, A. Ghestem, E. Ismailova, T. Hervé, S. Sanaur, C. Bernard, G. G. Malliaras, *Nat. Commun.* **2013**, *4*, 1575.
[11] Y. Zhang, J. Li, R. Li, D.-T. Sbircea, A. Giovannitti, J. Xu, H. Xu, G. Zhou, L. Bian, I. McCulloch, N. Zhao, *ACS Appl. Mater. Interfaces* **2017**, *9*, 38687.
[12] Y. van de Burgt, E. Lubberman, E. J. Fuller, S. T. Keene, G. C. Faria, S. Agarwal, M. J. Marinella, A. A. Talin, A. Salleo, *Nat. Mater.* **2017**, *16*, 414.
[13] P. Gkoupidenis, N. Schaefer, B. Garlan, G. G. Malliaras, *Adv. Mater.* **2015**, *27*, 7176.
[14] P. Gkoupidenis, N. Schaefer, X. Strakosas, J. A. Fairfield, G. G. Malliaras, *Appl. Phys. Lett.* **2016**, *107*, 263302.
[15] P. Gkoupidenis, D. A. Koutsouras, G. G. Malliaras, *Nat. Commun.* **2017**, *8*, 15448.
[16] D. Nilsson, N. Robinson, M. Berggren, R. Forchheimer, *Adv. Mater.* **2005**, *17*, 353.
[17] D. Nilsson, M. Chen, T. Kugler, T. Remonen, M. Armgarth, M. Berggren, *Adv. Mater.* **2002**, *14*, 51.
[18] K. Tybrandt, K. C. Larsson, A. Richter-Dahlfors, M. Berggren, *Proc. Natl. Acad. Sci. USA* **2010**, *107*, 9929.
[19] P. C. Hütter, T. Rothländer, G. Scheipl, B. Stadlober, *IEEE Trans. Electron Devices* **2015**, *62*, 4231.
[20] P. Andersson, D. Nilsson, P.-O. Svensson, M. Chen, A. Malmström, T. Remonen, T. Kugler, M. Berggren, *Adv. Mater.* **2002**, *14*, 1460.
[21] R. Mannerbro, M. Ranlöf, N. Robinson, R. Forchheimer, *Synth. Methods* **2008**, *158*, 556.
[22] D. Braga, N. C. Erickson, M. J. Renn, R. J. Holmes, C. D. Frisbie, *Adv. Funct. Mater.* **2012**, *22*, 1623.
[23] Y. Xu, C. Liu, D. Khim, Y.-Y. Noh, *Phys. Chem. Chem. Phys.* **2015**, *17*, 26553.
[24] K.-J. Baeg, M. Caironi, Y.-Y. Noh, *Adv. Mater.* **2013**, *25*, 4210.
[25] D. Vanmaekelbergh, A. J. Houtepen, J. J. Kelly, *Electrochim. Acta* **2007**, *53*, 1140.

[26] N. D. Robinson, P.-O. Svensson, D. Nilsson, M. Berggren, *J. Electrochem. Soc.* **2006**, *153*, H39.
[27] D. A. Bernards, G. G. Malliaras, *Adv. Funct. Mater.* **2007**, *17*, 3538.
[28] F. Cicoira, M. Sessolo, O. Yaghmazadeh, J. A. DeFranco, S. Y. Yang, G. G. Malliaras, *Adv. Mater.* **2010**, *22*, 1012.
[29] J. T. Friedlein, M. J. Donahue, S. E. Shaheen, G. G. Malliaras, R. R. McLeod, *Adv. Mater.* **2016**, *28*, 8398.
[30] J. Rivnay, P. Leleux, M. Sessolo, D. Khodagholy, T. Hervé, M. Fiocchi, G. G. Malliaras, *Adv. Mater.* **2013**, *25*, 7010.
[31] S. P. White, K. D. Dorfman, C. D. Frisbie, *J. Phys. Chem. C* **2016**, *120*, 108.
[32] A. Giovannitti, D.-T. Sbircea, S. Inal, C. B. Nielsen, E. Bandiello, D. A. Hanifi, M. Sessolo, G. G. Malliaras, I. McCulloch, J. Rivnay, *Proc. Natl. Acad. Sci. USA* **2016**, *113*, 12017.
[33] C. B. Nielsen, A. Giovannitti, D.-T. Sbircea, E. Bandiello, M. R. Niazi, D. A. Hanifi, M. Sessolo, A. Amassian, G. G. Malliaras, J. Rivnay, I. McCulloch, *J. Am. Chem. Soc.* **2016**, *138*, 10252.
[34] A. Giovannitti, C. B. Nielsen, D.-T. Sbircea, S. Inal, M. Donahue, M. R. Niazi, D. A. Hanifi, A. Amassian, G. G. Malliaras, J. Rivnay, I. McCulloch, *Nat. Commun.* **2016**, *7*, 13066.
[35] S. Inal, J. Rivnay, P. Leleux, M. Ferro, M. Ramuz, J. C. Brendel, M. M. Schmidt, M. Thelakkat, G. G. Malliaras, *Adv. Mater.* **2014**, *26*, 7450.
[36] G. Tarabella, C. Santato, S. Y. Yang, S. Iannotta, G. G. Malliaras, F. Cicoira, *Appl. Phys. Lett.* **2010**, *97*, 123304.
[37] O. Larsson, A. Laiho, W. Schmickler, M. Berggren, X. Crispin, *Adv. Mater.* **2011**, *23*, 4764.
[38] S. Fabiano, S. Braun, M. Fahlman, X. Crispin, M. Berggren, *Adv. Funct. Mater.* **2014**, *24*, 695.
[39] L. Kergoat, L. Herlogsson, B. Piro, M. C. Pham, G. Horowitz, X. Crispin, M. Berggren, *Proc. Natl. Acad. Sci. USA* **2012**, *109*, 8394.
[40] M. Braendlein, T. Lonjaret, P. Leleux, J.-M. Badier, G. G. Malliaras, *Adv. Sci.* **2017**, *4*, 1600247.
[41] M. Schell, F. N. Albahadily, J. Safar, Y. Xu, *J. Phys. Chem.* **1989**, *93*, 4806.
[42] G. Samjeské, A. Miki, S. Ye, A. Yamakata, Y. Mukouyama, H. Okamoto, M. Osawa, *J. Phys. Chem. B* **2005**, *109*, 23509.
[43] D. Khodagholy, J. Rivnay, M. Sessolo, M. Gurfinkel, P. Leleux, L. H. Jimison, E. Stavrinidou, T. Herve, S. Sanaur, R. M. Owens, G. G. Malliaras, *Nat. Commun.* **2013**, *4*, 2133.